Spontaneous spin accumulation in singlet-triplet Josephson junctions

K. Sengupta[1] and Victor M. Yakovenko[2]

[1]*TCMP division, Saha Institute of Nuclear Physics, 1/AF Bidhannagar, Kolkata-700064, India*
[2]*Joint Quantum Institute and Center for Nanophysics and Advanced Materials,*
Department of Physics, University of Maryland, College Park, Maryland 20742-4111, USA
(Dated: v.10, edited by VMY 12 September 2008, compiled February 27, 2009)

We study the Andreev bound states in a Josephson junction between a singlet and a triplet superconductors. Because of the mismatch in the spin symmetries of pairing, the energies of the spin up and down quasiparticles are generally different. This results in imbalance of spin populations and net spin accumulation at the junction in equilibrium. This effect can be detected using probes of local magnetic field, such as the scanning SQUID, Hall, and Kerr probes. It may help to identify potential triplet pairing in $(TMTSF)_2X$, Sr_2RuO_4, and oxypnictides.

Superconductivity with unconventional pairing, particularly spin-triplet pairing, attracts a lot of interest in the condensed matter physics community and beyond. There is significant experimental evidence in favor of triplet pairing in the quasi-one-dimensional (Q1D) organic superconductors $(TMTSF)_2X$ [1, 2], ruthenate Sr_2RuO_4 [3], and some heavy-fermion materials. In the recently discovered oxypnictide superconductors [4], some experiments (observation of zero-bias conductance peak in tunneling [5] and H_{c_2} exceeding the Pauli paramagnetic limit [6]) suggest a possible triplet pairing. Triplet [7] and singlet [8] pairings were proposed in different theoretical models of oxypnictides. However, triplet pairing is not firmly established in any these materials. In this paper, we propose a new physical effect, which can provide useful information about spin symmetry of superconducting pairing. We predict that electron spin accumulation should spontaneously develop at an interface between a singlet and a triplet superconductors. Other methods for detection of triplet pairing using superconducting junctions were proposed in Refs. [9, 10].

The predicted spin accumulation originates from the Andreev bound states at the interface between the singlet and triplet superconductors. Because of the mismatch between the spin symmetries of pairing, the spin up and down Andreev bound states have different energies. This results in different population of the spin up and down states and net spin accumulation at the interface. The preferred axis for the spin projection is determined by the vector $\boldsymbol{d}$ of the triplet pairing, and the sign of the accumulated spin is determined by spontaneous symmetry breaking. The resulting magnetization can be detected using local probes of magnetic field, such as the scanning SQUID, Hall, or Kerr probes. If a voltage V is applied to the junction, then the magnetization would oscillate with the Josephson frequency $2eV/\hbar$. In this paper, we present calculations in two cases: for the non-chiral p_x-wave pairing, relevant to the $(TMTSF)_2X$ materials [11], and for the chiral $p_x + ip_y$ pairing, relevant to Sr_2RuO_4 [12]. For oxypnictides, the calculations would be more complicated because of the multiple bands [8], but the result should be qualitatively the same. Although the Andreev bound states [13] in the singlet-triplet Josephson junctions [14] were studied in literature before, the spin accumulation effect was not recognized, except in Ref. [15] for the special case of equal energy gaps.

Let us consider a Josephson junction between an s-wave and a p-wave superconductors located at $x < 0$ and $x > 0$ respectively, as shown in Fig. 1. The two superconductors are separated by a narrow insulating barrier at $x = 0$, which is modeled by the delta-function potential $U(x) = U_0\delta(x)$. The interface between the superconductors is assumed to be smooth, so that the electron momentum parallel to the interface $\boldsymbol{k}_\parallel = (k_y, k_z)$ is a good quantum number. The interface plane is perpendicular to the planes of Sr_2RuO_4 or chains of $(TMTSF)_2X$, as shown in Fig. 1. The pairing potential of the singlet s-wave superconductor on the left (L) side is

$$\langle \hat{c}_{\boldsymbol{k},\sigma}\hat{c}_{-\boldsymbol{k},\bar{\sigma}}\rangle \propto \Delta_1 \mathrm{sgn}(\sigma) \equiv \Delta^L_\sigma, \qquad (1)$$

where $\hat{c}_{\boldsymbol{k},\sigma}$ is the destruction operator of an electron with the momentum $\boldsymbol{k}$ and spin $\sigma = \uparrow, \downarrow$. Here, $\mathrm{sgn}(\sigma) = +(-)$ and $\bar{\sigma} = \downarrow (\uparrow)$ for $\sigma = \uparrow (\downarrow)$. The pairing potential of the triplet p-wave superconductor on the right (R) side is

$$\langle \hat{c}_{\boldsymbol{k},\sigma}\hat{c}_{-\boldsymbol{k},\sigma'}\rangle \propto \Delta_2\, i\hat{\sigma}_y(\hat{\boldsymbol{\sigma}} \cdot \boldsymbol{d})\, f(\boldsymbol{k})\, e^{i\phi_0}. \qquad (2)$$

Here $\hat{\boldsymbol{\sigma}}$ are the Pauli matrices in the spin space, $\boldsymbol{d}$ is a unit vector characterizing the spin polarization of the triplet superconductor, and ϕ_0 is the U(1) phase difference across the junction. The function $f(\boldsymbol{k})$ represents the orbital symmetry of the pairing potential: $f(\boldsymbol{k}) = (k_x + ik_y)/k_F$ for the chiral $p_x + ip_y$ pairing and $f(\boldsymbol{k}) = k_x/k_F$ for the non-chiral p_x pairing, where k_F is the Fermi momentum. We assume that the vector $\boldsymbol{d}$ has a uniform orientation independent of $\boldsymbol{k}$. By selecting the spin quantization axis $\hat{z}$ along $\boldsymbol{d}$, Eq. (2) is simplified as

$$\langle \hat{c}_{\boldsymbol{k},\sigma}\hat{c}_{-\boldsymbol{k},\bar{\sigma}}\rangle \propto \Delta_2\, f(\boldsymbol{k})\, e^{i\phi_0} \equiv \Delta^R_\sigma. \qquad (3)$$

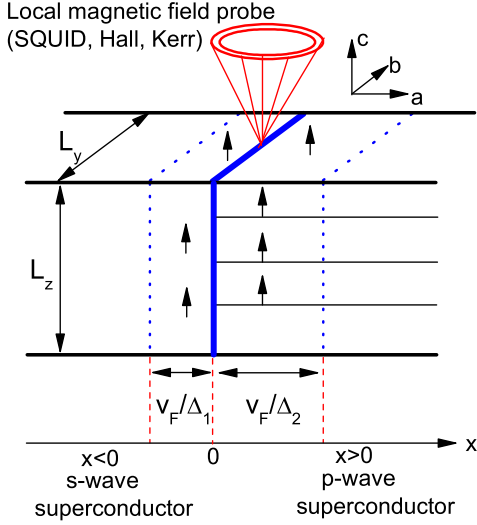In this representation, both singlet (1) and triplet (3) pairing potentials couple electrons with opposite spins.

FIG. 1: A Josephson junction between a single and a triplet superconductors. The thin black solid lines represent chains for $(TMTSF)_2X$ or planes for Sr_2RuO_4. The blue dotted lines indicates the localization lengths of the Andreev bound states. The cone represents a probe of the local magnetic field produced by spin accumulation at the interface.

Electron states in a superconductor are described by the Bogoliubov operators $\hat{\gamma}$, which are related to the electron operators $\hat{c}$ by the following equations [16]

$$\hat{\gamma}_{\sigma n \boldsymbol{k}_\parallel} = \int dx \, [u^*_{\sigma n \boldsymbol{k}_\parallel}(x) \, \hat{c}_{\sigma \boldsymbol{k}_\parallel}(x) + v^*_{\sigma n \boldsymbol{k}_\parallel}(x) \, \hat{c}^\dagger_{\bar{\sigma}\bar{\boldsymbol{k}}_\parallel}(x)], \quad (4)$$

$$\hat{c}_{\sigma \boldsymbol{k}_\parallel}(x) = \sum_n [u_{\sigma n \boldsymbol{k}_\parallel}(x) \, \hat{\gamma}_{\sigma n \boldsymbol{k}_\parallel} + v^*_{n \bar{\sigma}\bar{\boldsymbol{k}}_\parallel}(x) \, \hat{\gamma}^\dagger_{n \bar{\sigma}\bar{\boldsymbol{k}}_\parallel}], \quad (5)$$

where $\bar{\boldsymbol{k}}_\parallel = -\boldsymbol{k}_\parallel$, and n is the quantum number of the Bogoliubov eigenstates. The two-component wave functions $\psi_{\sigma n}(x, \boldsymbol{k}_\parallel) = [u_{\sigma n \boldsymbol{k}_\parallel}(x), v_{\sigma n \boldsymbol{k}_\parallel}(x)]$ are the eigenstates of the Bogoliubov-de Gennes (BdG) equation with the eigenenergies $E_{\sigma n \boldsymbol{k}_\parallel}$

$$\begin{pmatrix} \hat{H}_0 + U(x) & \Delta_\sigma(x, \hat{k}_x, \boldsymbol{k}_\parallel) \\ \Delta^*_\sigma(x, \hat{k}_x, \boldsymbol{k}_\parallel) & -\hat{H}_0 - U(x) \end{pmatrix} \psi_\sigma(x) = E_\sigma \psi_\sigma(x), \quad (6)$$

where we omitted the labels n and $\boldsymbol{k}_\parallel$ for ψ and E to shorten notation. Here $\hat{H}_0 = \varepsilon(\hat{k}_x, \boldsymbol{k}_\parallel) - \mu$ is the electron dispersion relation with $\hat{k}_x = -i\partial_x$ and the chemical potential μ, and we set $\hbar = 1$. In Sr_2RuO_4, the main Fermi surface is circular, so we take $\varepsilon = (k_x^2 + k_y^2)/2m$, where m is the effective mass. In Q1D conductors, the Fermi surface consists of two open sheets perpendicular to the chains, so we take $\varepsilon = k_x^2/2m - t_b \cos(bk_y) - t_c \cos(ck_z)$, where the first term represents motion along the chains, and t_b, t_c, b, and c are the interchain tunneling amplitudes and spacings [17]. Notice that the spin projection σ is a good quantum number for the Bogoliubov quasiparticles (4), and the BdG equations (6) separate for $\sigma = \uparrow$

and $\downarrow$. The pairing potential Δ_σ in Eq. (6) is given by Eq. (1) for $x < 0$ and by Eq. (3) for $x > 0$.

The wave functions ψ^L_σ and ψ^R_σ on the left and right sides of the junction satisfy the standard boundary condition at $x = 0$ obtained by integrating Eq. (6) over x from -0 to $+0$

$$\psi^R_\sigma(0) = \psi^L_\sigma(0), \; (\partial_x \psi^R_\sigma - \partial_x \psi^L_\sigma)_{x=0} = 2mU_0 \psi^L_\sigma(0). \quad (7)$$

We are interested in the subgap bound states of Eq. (6) with energies $|E| \leq \text{Min}[\Delta_1, \Delta_2]$, which are localized near the junction. Such localized solutions can be obtained as a superposition of the wavefunctions for the right and left moving quasiparticles [15]:

$$\psi^\beta_\sigma(x) = e^{-\kappa^\beta_\sigma x} \left[A^\beta e^{i\tilde{k}_F x} \begin{pmatrix} u^\beta_{\sigma+} \\ v^\beta_{\sigma+} \end{pmatrix} + B^\beta e^{-i\tilde{k}_F x} \begin{pmatrix} u^\beta_{\sigma-} \\ v^\beta_{\sigma-} \end{pmatrix} \right]. \quad (8)$$

Here the superscript $\beta = R, L$ labels the wave functions on the right and left sides of the junction. The subscript $\alpha = \pm$ in $u_{\sigma\alpha}$ or $v_{\sigma\alpha}$ denotes the right ($\alpha = +$) or left ($\alpha = -$) moving quasiparticles. The parameters $\kappa^{R(L)}_\sigma = +(-)\sqrt{\Delta^2_{2(1)} - E^2_\sigma}/\tilde{v}_F$ determine the inverse localization lengths of the bound states inside the right and left superconductors. The variables $\tilde{k}_F$ and $\tilde{v}_F$ are the x components of the Fermi momentum and Fermi velocity, which, generally, depend on $\boldsymbol{k}_\parallel$. For Sr_2RuO_4, $\tilde{k}_F = \sqrt{k_F^2 - k_y^2}$ and $\tilde{v}_F = \tilde{k}_F/m$. For Q1D conductors, $\tilde{k}_F = k_F + 2t_b \cos(bk_y)/v_F + 2t_c \cos(ck_z)/v_F$ and $\tilde{v}_F \approx v_F$, where $v_F = k_F/m$. The coefficients $u^\beta_{\sigma\alpha}$ and $v^\beta_{\sigma\alpha}$ are determined by substituting the right and left moving terms into Eq. (6) away from the junction. They satisfy

$$\eta^\beta_{\sigma\alpha} = \frac{u^\beta_{\sigma\alpha}}{v^\beta_{\sigma\alpha}} = \frac{E_\sigma - i \, \text{sgn}(\alpha) \, \tilde{v}_F \kappa^\beta_\sigma}{\Delta^\beta_\sigma}, \quad (9)$$

where Δ^β_σ are given by Eqs. (1) and (3). Notice that all variables in Eqs. (8) and (9), generally, depend on $\boldsymbol{k}_\parallel$.

Substituting Eq. (8) into Eq. (7), we obtain a set of 4 linear homogeneous equations for the coefficients A^β and B^β. A condition for non-zero solutions requires vanishing of the determinant of the corresponding 4×4 matrix, which yields the following equation

$$\frac{(\eta^R_{\sigma+} - \eta^L_{\sigma+})(\eta^R_{\sigma-} - \eta^L_{\sigma-})}{(\eta^R_{\sigma-} - \eta^L_{\sigma+})(\eta^R_{\sigma+} - \eta^L_{\sigma-})} = 1 - D(\boldsymbol{k}_\parallel). \quad (10)$$

Here $D(\boldsymbol{k}_\parallel) = 4/(4 + Z^2(\boldsymbol{k}_\parallel))$ is the transmission coefficient of the barrier. For Q1D conductors, $Z(\boldsymbol{k}_\parallel) = Z_0 = 2U_0/v_F$ is independent of the transverse momentum. For Sr_2RuO_4, $Z(\boldsymbol{k}_\parallel) = Z_0 k_F/\sqrt{k_F^2 - k_y^2}$. Substituting Eq. (9) into Eq. (10), we obtain an equation for the energies of the Andreev bound states

$$\mathcal{A} \sin(\Phi_{\boldsymbol{k}_\parallel}) - \mathcal{B} \cos(\Phi_{\boldsymbol{k}_\parallel}) = \text{sgn}(\sigma) \sin(\phi_0) D(\boldsymbol{k}_\parallel). \quad (11)$$
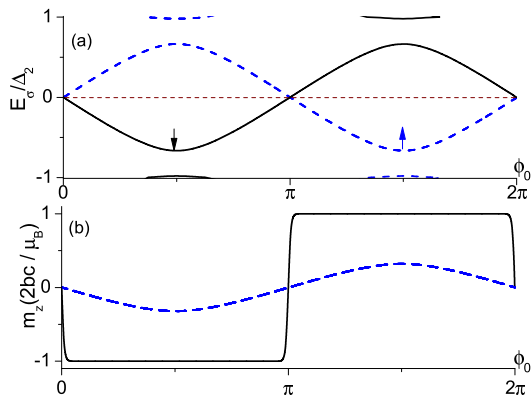
FIG. 2: (a) The energies $E_\uparrow$ (dashed lines) and $E_\downarrow$ (solid lines) of the Andreev bound states vs. the phase ϕ_0 between the s and p_x-wave superconductors ($D = 0.8$ and $\Delta_2 = 0.5\Delta_1$). (b) Magnetic moment m_z per unit area of the interface, Eq. (12), vs. ϕ_0 for $T/\Delta_2 = 0.01$ (solid line) and 1 (dashed line).

FIG. 3: The energies $E_\uparrow(k_y)$ (blue dotted lines) and $E_\downarrow(k_y)$ (red dash-dotted lines) vs. k_y for the phase $\phi_0 = \pi/2$ between the s and $p_x + ip_y$ superconductors ($Z_0 = 1$). For $\phi_0 = 0$ and π, $E_\uparrow(k_y) = E_\downarrow(k_y)$ is shown by the black solid line.

Here $\phi(\boldsymbol{k})$ is the phase of the function $f(\boldsymbol{k})$ in Eq. (3), and $\Phi_{\boldsymbol{k}_\parallel} = [\phi(\tilde{k}_F, \boldsymbol{k}_\parallel) - \phi(-\tilde{k}_F, \boldsymbol{k}_\parallel)]/2$ is a half of the phase difference between the points on the Fermi surface connected by specular reflection from the barrier, selected so that $0 \le \Phi \le \pi$ [12]. The coefficients $\mathcal{A}$ and $\mathcal{B}$ are

$$\mathcal{A} = [2 - D(\boldsymbol{k}_\parallel)]\,\epsilon_{\sigma 1}\sqrt{1 - \epsilon_{\sigma 2}^2} + D(\boldsymbol{k}_\parallel)\,\epsilon_{\sigma 2}\sqrt{1 - \epsilon_{\sigma 1}^2},$$

$$\mathcal{B} = -D(\boldsymbol{k}_\parallel)\,\epsilon_{\sigma 1}\,\epsilon_{\sigma 2} + [2 - D(\boldsymbol{k}_\parallel)]\sqrt{(1 - \epsilon_{\sigma 1}^2)(1 - \epsilon_{\sigma 2}^2)}.$$

where $\epsilon_{\sigma 1(2)} = E_\sigma(\boldsymbol{k}_\parallel; \phi_0)/\Delta_{1(2)} \le 1$ is the dimensionless energy of the bound state. In the case $\Delta_1 = \Delta_2$, the equations simplify and reproduce the results of Ref. [15].

Notice that E_σ depends on the spin index σ only through the right-hand side of Eq. (11), which is invariant under the transformation $\sigma \to \bar{\sigma}$ and $\phi_0 \to \phi_0 + \pi$, so $E_\sigma(\boldsymbol{k}_\parallel; \phi) = E_{\bar{\sigma}}(\boldsymbol{k}_\parallel; \phi + \pi)$. This relation can be understood by noting that the singlet pairing potential (1) has opposite signs for $\sigma = \uparrow$ and $\downarrow$, whereas the triplet pairing potential (3) has the same sign. So, a phase difference ϕ_0 across the junction for spin-up quasiparticles implies the effective phase difference $\phi_0 + \pi$ for spin-down quasiparticles, which explains the above-mentioned invariance. We see that the bound states energies $E_\uparrow$ and $E_\downarrow$ are generally different for a given ϕ_0, which is the key point for understanding of spin accumulation [18].

For the p_x-wave pairing, we have $f(-k_F) = -f(k_F)$, so $\Phi_{\boldsymbol{k}_\parallel} = \pi/2$, and Eq. (11) reduces to $\mathcal{A} = D\,\text{sgn}(\sigma)\sin(\phi_0)$, where $D = 4/(4 + Z_0^2)$. In this case, the energies E_σ are independent of $\boldsymbol{k}_\parallel$ and are plotted vs. ϕ_0 in Fig. 2a. Depending on ϕ_0, there are two or four of such states for each $\boldsymbol{k}_\parallel$. The spin up and down bound states have opposite energies $E_\uparrow = -E_\downarrow$, as shown by the dashed and solid lines in Fig. 2a. The difference between the Fermi populations of the spin up and down states gives a net
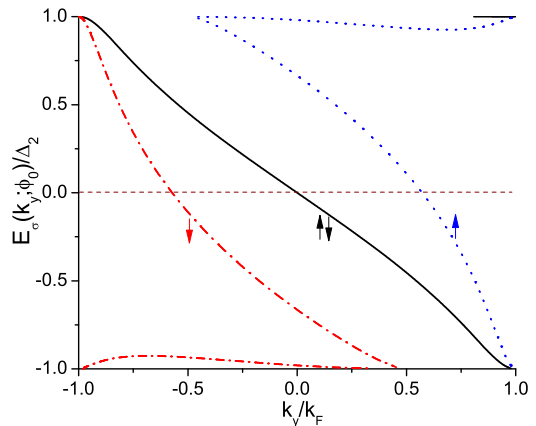
magnetic moment m_z per unit area of the interface [20]

$$m_z = \frac{\mu_B}{2bc}\tanh\left(\frac{E_\downarrow(\phi_0)}{2T}\right), \qquad (12)$$

where μ_B is the Bohr magneton, T is the temperature, and the prefactor $1/2$ compensates for double-counting [11, 15]. A plot of m_z vs. ϕ_0 is shown in Fig. 2b for two different temperatures. At low T, the magnetic moment is close to $\mu_B/2$ per chain, since only the lower energy state is populated. In an open circuit, the value of the phase ϕ_0 is determined by minimization of the total energy of the system. For the energy levels shown in Fig. 2a, the minimum is achieved at either $\phi_0 = \pi/2$ or $\phi_0 = 3\pi/2$ (the same as $\phi_0 = -\pi/2$) [19]. The system spontaneously breaks the symmetry and selects one of the two energy minima with negative or positive magnetization.

For the chiral $p_x + ip_y$ pairing, we have $\phi(\boldsymbol{k}) = \arctan(k_y/k_x)$ and $\Phi_{\boldsymbol{k}_\parallel} = \phi(k_y) + \pi/2$, so that $\sin\Phi_{\boldsymbol{k}_\parallel} = |k_x|/k_F$ and $\cos\Phi_{\boldsymbol{k}_\parallel} = -k_y/k_F$. Then, Eq. (11) gives the energies $E_\sigma(k_y; \phi_0)$ dependent on the transverse momentum k_y because of the broken time-reversal symmetry. The plot of $E_\sigma(k_y; \phi_0)$ vs. k_y for several values of ϕ_0 is shown in Fig. 3. The energy splitting between $E_\uparrow$ and $E_\downarrow$ is maximal at $\phi_0 = \pm\pi/2$ and vanishes at $\phi_0 = 0$ and π. The imbalance between the spin up and down populations produces the net magnetic moment m_z per unit area of the interface

$$m_z = \frac{\mu_B}{2c}\sum_{\sigma=\uparrow,\downarrow}\text{sgn}(\sigma)\int_{-k_F}^{k_F}\frac{dk_y}{2\pi}\,n_F\left(\frac{E_\sigma(k_y; \phi_0)}{T}\right), \quad (13)$$

where n_F is the Fermi distribution function, and c is the interplane distance for Sr_2RuO_4 [20]. The plot of m_z vs. ϕ_0 is shown in Fig. 4 for two different temperatures. The minimum of energy is achieved at $\phi_0 = \pm\pi/2$, so the
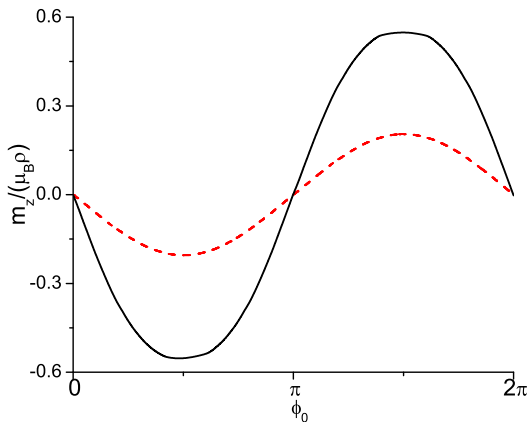
FIG. 4: Normalized magnetic moment m_z per unit area of the interface, Eq. (13), vs. ϕ_0 for $T = 0.01\Delta_2$ (solid line) and $T = \Delta_2$ (dashed line) for a junction between the s and $p_x + ip_y$ superconductors ($\rho = k_F/2\pi c$).

system spontaneous breaks the symmetry and selects one of the two optimal values for ϕ_0.

Figs. 2b and 4 show that the magnetic moment m_z changes sign when ϕ_0 crosses π. If a bias voltage V is applied across the junction, it would make the phase difference time-dependent: $\phi_0(t) = 2eVt$. Then, the magnetization m_z at the interface would oscillate with the time period π/eV. We assume that the oscillations are slow enough for the spin population to remain close to the thermal equilibrium at each moment of time.

Finally, we discuss possible experiments for detection of the spontaneous spin polarization. A schematic experimental setup is shown in Fig. 1. Assuming semi-infinite geometry in the z direction, the magnetization at the junction and the magnetic field can be estimated as $B \simeq \mu_0 \mu_B \rho \kappa/4$, where $\kappa \simeq \Delta_2/v_F$ is the inverse penetration depth of the bound states in the case $\Delta_1 \gg \Delta_2$, $\rho = 1/bc$ for (TMTSF)$_2$X, and $\rho = k_F/2\pi c$ for Sr$_2$RuO$_4$. This magnetic field can be measured using a scanning SQUID or Hall microscope [21, 22]. For (TMTSF)$_2$X, we have $b = 0.77$ nm, $c = 1.35$ nm and $\kappa^{-1} \simeq 0.6$ μm, which gives $B \simeq 0.3$ G and a magnetic flux $0.06\Phi_0$ (where $\Phi_0 = hc/2e$) through a square scanning SQUID loop of the size $l = 10$ μm. For Sr$_2$RuO$_4$, we have $k_F = 7.5 \times 10^{-9}$ m^{-1}, $\kappa^{-1} = 66$ nm and $c = 1.3$ nm, which gives the field 0.7 G and the flux $0.15\Phi_0$. The estimated magnetic fields are well above the typical Hall-probe sensitivity of 80 mG at 1 Hz [21]. However, chiral superconductors are also expected to have an additional magnetic field due to the charge currents carried by the chiral Andreev bound states [23]. A Josephson junction between Au$_{0.5}$In$_{0.5}$ and Sr$_2$RuO$_4$ was scanned using the SQUID and Hall probes in Ref. [22], but no spontaneous magnetic field was detected. A reason for the negative experimental result remains an open question. Local magnetization can be also detected optically using the Kerr angle rotation [24]. This effect was observed in Ref. [25] in the bulk of Sr$_2$RuO$_4$ due to the orbital time-reversal symmetry breaking in the $p_x + ip_y$ state. However, the Kerr experiment has not been performed in a scanning mode at a junction with a singlet superconductor.

In conclusion, we have shown that a Josephson junction between a singlet and a triplet superconductors should exhibit spontaneous spin accumulation due to mismatch of the spin pairing symmetries. The vector of the accumulated spin points along the vector $\boldsymbol{d}$ of the triplet superconductor. The sign and magnitude of the spin depend on the phase difference ϕ_0 between the superconductors. In equilibrium, the system spontaneously breaks symmetry and selects one of the two values of ϕ_0 that minimize total energy and maximize spin accumulation. When a bias voltage V is applied to the junctions, the accumulated spin oscillates in time. The magnetic field produced by the accumulated spin can be detected using the SQUID, Hall, or Kerr local probes.

---

[1] TMTSF stands for tetramethyltetraselenafulvalene and X represents inorganic anions such PF$_6$ or ClO$_4$.
[2] I.J. Lee et al., Phys. Rev. Lett. **78**, 3555 (1997); ibid. **88**, 017004 (2001); Phys. Rev. B **62**, R14669 (2000).
[3] Y. Maeno, T.M. Rice, and M. Sigrist, Phys. Today **54** (1), 42 (2001); **54** (3), 104 (2001); A.P. Mackenzie and Y. Maeno, Rev. Mod. Phys. **75**, 657 (2003).
[4] Y. Kamihara et al., J. Am. Chem. Soc. **130**, 3296 (2008); G.F. Chen et al., Phys. Rev. Lett. **101**, 057007 (2008).
[5] L. Shan et al., Europhys. Lett. **83**, 57004 (2008).
[6] F. Hunte et al., Nature **453**, 903 (2008).
[7] G. Xu et al., Europhys. Lett. **82**, 67002 (2008); P.A. Lee and X.-G. Wen, arXiv:0804.1739.
[8] I.I. Mazin et al., Phys. Rev. Lett. **101**, 057003 (2008); K. Kuroki et al., Phys. Rev. Lett. **101**, 087004 (2008).
[9] Y. Tanaka et al., Phys. Rev. Lett. **99**, 037005 (2007).
[10] Y. Asano et al., Phys. Rev. Lett. **99**, 067005 (2007).
[11] K. Sengupta et al., Phys. Rev. B **63**, 144531 (2001).
[12] K. Sengupta, H.-J. Kwon, and V.M. Yakovenko, Phys. Rev. B **65**, 104504 (2002).
[13] Y. Asano et al., Phys. Rev. B **67**, 184505 (2003).
[14] S. Yip, J. Low Temp. Phys. **91**, 203 (1993); N. Yoshida et al., ibid. **117**, 563 (1999); Y. Asano et al., Phys. Rev. B **71**, 214501 (2005).
[15] H.-J. Kwon, K. Sengupta, and V.M. Yakovenko, Eur. Phys. J. B **37**, 349 (2004).
[16] A.M. Zagoskin, Quantum Theory of Many-Body Systems (Springer, New York, 1998).
[17] We omit the interplane tunneling term $t_c \cos(ck_z)$ for Sr$_2$RuO$_4$, because it drops out like for Q1D conductors.
[18] The Andreev bound states (8) carry zero spin current, so there is no spin supercurrent through the junction.
[19] Somewhat similar behavior was also found for a junction between even- and odd-frequency superconductors [9].
[20] Eqs. (12) and (13) omit contributions from states at the edge of the gap, which have large localization lengths.
[21] P.G. Bjornsson et al., Phys. Rev. B **72**, 012504 (2005).
[22] J.R. Kirtley et al., Phys. Rev. B **76**, 014526 (2007).
[23] H-J. Kwon, K. Sengupta, and V. M. Yakovenko, Synth. Metals **133-134**, 27 (2003).

[24] V. Sih *et al.*, Nature Phys. **1**, 31 (2005).
[25] J. Xia *et al.*, Phys. Rev. Lett. **97**, 167002 (2006).